

Neutron Investigation of the Ion Dynamics in Liquid Mercury: Evidence for Collective Excitations

L. E. Bove,¹ F. Sacchetti,¹ C. Petrillo,² B. Dorner,³ F. Formisano,⁴ and F. Barocchi⁵

¹*INFN and Dipartimento di Fisica, Università di Perugia, I-06123 Perugia, Italy*

²*INFN and Dipartimento di Fisica, Politecnico di Milano, I-20133 Milano, Italy*

³*Institut Laue Langevin, B.P. 156, F-38042 Grenoble Cedex 09, France*

⁴*INFN, OGG-Grenoble, B.P. 156, F-38042 Grenoble Cedex 09, France*

⁵*INFN and Dipartimento di Fisica, Università di Firenze, I-50125 Firenze, Italy*

(Received 4 August 2001; published 2 November 2001)

The ion dynamics of liquid mercury was investigated by inelastic neutron scattering. By exploiting an optimized high-resolution (~ 1 meV) experimental configuration, the dynamic response function was accurately measured. Collective excitations extending up to 0.6 \AA^{-1} were observed with an associated velocity of 2100 ± 80 m/s. This value is notably greater than the sound velocity, but it is provided by a simple Bohm-Staver calculation. The latter finding emphasizes those electron-related features in the ion dynamics, which are common to systems as different as polyvalent and alkali metals.

DOI: 10.1103/PhysRevLett.87.215504

PACS numbers: 61.12.-q, 61.25.Mv, 71.10.Ca

Investigation of the dynamic behavior of liquid metals at the atomic scale is of considerable interest because of those peculiar features in the excitation spectra that can no longer be interpreted by extending the description of the liquid from classical hydrodynamics [1]. The microscopic region is, indeed, characterized by the occurrence of collective excitations, i.e., propagating ion density fluctuations, which exhibit a dispersion relation extending over a relatively wide range of momentum transfers [2–8] (typically, up to half the position of the first maximum of the static structure factor). Understanding the microscopic mechanisms responsible for the propagation and the decay of these correlated ionic motions is still a challenge in liquid metals, where the dynamic behavior cannot be disentangled by the interacting electron gas effects [1,6,8]. A recent x-ray inelastic scattering experiment [8] on the low-electron-density liquid metal $\text{Li}(\text{NH}_3)_4$ has shown that long-living ion density fluctuations exist with a dispersion curve which is dramatically affected by the electron-electron interactions. The analysis of collective excitations, extending beyond the hydrodynamic limit, represents an essential contribution to the development of meaningful and reliable theoretical models of the liquid state [9,10].

In a recent paper, we have investigated the ion dynamics of a properly tailored K-Cs liquid alloy [6] and shown that the dispersion curves measured in K-Cs, Rb [3], and Cs [4] at the melting point satisfy to a scaling relation which substantially reflects the scaling of the electron gas densities, according to the simple Bohm-Staver (BS) model for the coupled electron-ion plasma [11]. Therefore, at least in liquid alkali metals, the electron gas density appears to be a key parameter which enables a unified description of the collective ion dynamics. This experiment-founded result is also featured by molecular dynamics simulations based on the Price-Singwi-Tosi potential [10]. Despite the success of this interpretation, ap-

plication of BS-like models has been confined to alkali systems, that is to low-electron-density systems. Considering that the BS approach amounts to neglecting the repulsive core potential, by a treatment of the ions as dimensionless pointlike particles, and to a rather simplified description of the electron-screened ion-ion Coulomb interaction, we believe that the investigation of a high-electron-density liquid metal would be fundamental to understanding the role of the electron-density-related effects against the ion size in governing the propagation of the ion density fluctuations. To this aim, the ideal sample should have a high electron density coupled to a free-electron-like band structure. The two joined requirements lead to polyvalent systems with an *sp*-like conduction band. The experimental data in simple (*s*-like) and polyvalent (*sp*-like) liquid metals suggest that the occurrence of long-living collective excitations is favored in these systems and it is possibly related to the details of the long-range part of the interatomic potential. A neutron scattering investigation on liquid lead is available [12] and collective excitations were, indeed, observed up to wave-vector transfers as high as 1.2 \AA^{-1} . However, the limited number of existing measurements makes the explanation of these properties still an open question.

Among polyvalent monatomic metals, liquid mercury has two specific characteristics that make it an appealing candidate for an inelastic neutron scattering investigation, namely the high electron density, $r_s = 2.70$ (the dimensionless parameter r_s being defined as $\frac{1}{\rho} = \frac{4}{3}\pi r_s^3 a_0^3$, ρ the electron number density, and a_0 the Bohr radius), and the rather low value of the sound velocity [13] ($v_s = 1451$ m/s), which makes the kinematic constraints on the neutron measurement less tight. Notwithstanding these characteristics, no neutron or x-ray measurement of the dynamic response function in liquid mercury has been carried out so far. Indeed, the main experimental difficulty is brought about by the high neutron (and x ray, as well)

absorption cross section of mercury. However, recent neutron measurements of the dynamic response have been carried out successfully in liquid samples of Cs [4] and $K_{52}Cs_{48}$ [6], that is in systems characterized by low scattering power and high absorption cross sections. Therefore, the experimental investigation of liquid mercury can be performed at a comparable accuracy level, although the presence of a rather high incoherent contribution, which partly masks the collective coherent response, makes this experiment even more challenging. The study of mercury dynamics will enable us to describe the effects of the electron screening in the limit of high electron density and to clarify the relative role of the core repulsive potential and the electron-screened ion-ion interaction.

Room temperature measurements were carried out at the three-axis spectrometer IN1 installed at the High Flux Reactor of the Institut Laue Langevin (Grenoble, France) and operated without the hot source. The experimental configuration was optimized for good resolution/intensity performances. A constant analyzer energy setup, which allows for an easy normalization of the data on absolute scale, was preferred. Very tight collimations of $25'$, $20'$, $20'$, and $30'$ were employed from the reactor to the detector. A wide vertically focusing Cu(200) monochromator and a wide vertically focusing PG(004) analyzer were used. The fixed final wave vector was 4.5 \AA^{-1} , corresponding to $\sim 42 \text{ meV}$ analyzer energy. This value was selected as an adequate compromise between the need of reducing the absorption cross section of mercury while maintaining a good energy resolution. Exploiting the low background ensured by the 1 m diameter evacuated flight path around the sample, high quality data were collected down to 1° scattering angle with this instrument configuration. Despite the tight collimations, a rather high incoming intensity was available. The sample cell was a flat, vacuum tight, $7 \times 4 \times 0.065 \text{ cm}^3$ aluminum cell, with wall thickness of $\sim 0.5 \text{ mm}$. The sample was 99.999% pure mercury with natural isotopic composition. The scattered intensity from the sample was measured at seven wave-vector transfers Q , namely at $Q = 0.25, 0.3, 0.4, 0.6, 0.8, 1.0,$ and 1.2 \AA^{-1} . Accurate measurements of the background (the empty cell, the absorber, and the environment) were necessary since, although rather small, it represents a non-negligible contribution on the tails of the scattering function and in those positions with the analyzer close to the incoming beam. The resolution of the instrument was obtained by measuring the intensity diffused at $Q = 0.3 \text{ \AA}^{-1}$ by a 1.5 mm thick vanadium slab placed inside the sample cell. The sample transmission was measured by inserting a plastic attenuator on the incoming beam and it turned out to be $T = 0.454 \pm 0.001$. The measured data were normalized to the same monitor counts and the proper background subtraction was applied.

The background-free intensity contains the contribution of multiple scattering (MS) processes taking place inside the Hg sample and between the sample and the cell. The

latter processes were neglected because of the low scattering cross section of aluminum. In mercury MS is expected to be small; however, since a much higher accuracy is necessary to treat the data of this absorbing system, we applied an iterative procedure for the MS correction [14]. The procedure consists of an initial guess for the trial single scattering cross section, the calculation of the MS contribution, the subtraction of it from the experimental data, and the use of the MS-free experimental data as input of the next MS calculation cycle. The procedure was repeated until convergence. By observing that at the incoming neutron energies of the experiment the MS was dominated by processes at high wave vector, the trial cross section could be suitably described within the incoherent approximation [15]. The simplest representation was that provided by a continuous diffusion model, i.e., a Lorentzian function with full width at half maximum (FWHM) equal to $2DQ^2$, $D = 1.57 \times 10^{-5} \text{ cm}^2 \text{ s}^{-1}$ is the self-diffusion constant. Although a convenient trial function, the simple diffusion Lorentzian did not produce convergence since it was not sufficient to describe the overall structure of the cross section. We found that the features of the cross section could be reproduced only by the sum of at least two Lorentzian functions, describing the quasielastic single scattering cross section, and a smaller contribution representing the propagating collective modes. The instrument resolution function, as measured by the vanadium standard, was described by a Gaussian function with a FWHM equal to $\sim 1.16 \text{ meV}$, in excellent agreement with the resolution curve calculated according to [16].

The MS-corrected experimental dynamic structure factors are shown in Fig. 1 versus energy transfer and at some selected wave-vector transfers. The main features of the dynamic structure factor are a sharp resolution-limited quasielastic peak superimposed to a quasielastic signal much broader than the resolution and inelastic side peaks. The inelastic structures are apparent in the low- Q spectra, while the structure of the quasielastic signal is well visible in the high- Q spectrum shown in Fig. 1 together with the elastic resolution. An accurate and quantitative analysis is required to describe the different features of the self- and collective ion dynamics as they show up in the present experimental data. As a first approach, we preferred to resort to an empirical fitting of the data that has the advantage of being a rather simple procedure while retaining the essential features of the complex real dynamics in a phenomenological way. We modeled the dynamic structure factor $S(Q, \omega)$ by using the minimum possible number of Lorentzian functions, namely two, to describe the quasielastic contribution $S_{qe}(Q, \omega)$ and a damped harmonic oscillator (DHO) to describe the purely inelastic component $S_{inel}(Q, \omega)$. The decomposition of $S_{qe}(Q, \omega)$ into the sum of two Lorentzian functions was the simplest working solution which enabled fitting the data with a reduced number of free parameters. $S(Q, \omega)$ was given by the sum of $S_{qe}(Q, \omega)$ and $S_{inel}(Q, \omega)$, with

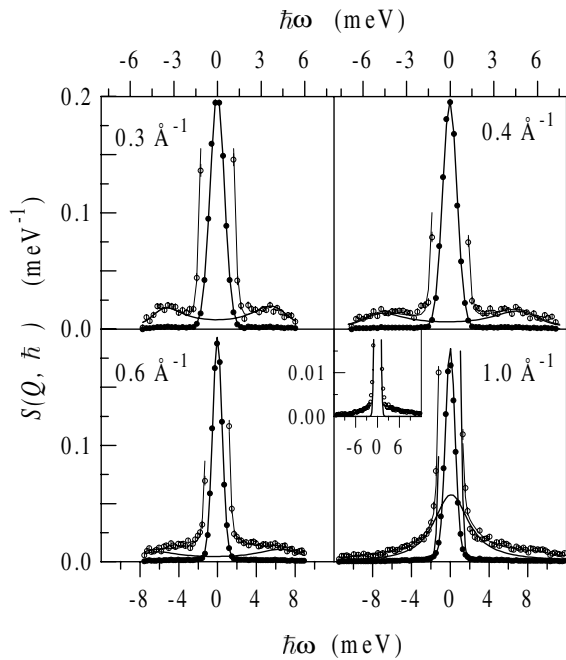


FIG. 1. Dynamic structure factor $S(Q, \hbar\omega)$ of liquid mercury versus energy transfer and at selected values of wave-vector transfers. The experimental data (dots) are also shown on a scale expanded by a factor of 10 (circles) to emphasize the inelastic structures. The full lines are the curves calculated according to the fitting model described in the text. Moreover, at $Q = 0.3, 0.4,$ and 0.6 \AA^{-1} the inelastic contribution (DHO) is shown, whereas at $Q = 1.0 \text{ \AA}^{-1}$ the two quasielastic (Lorentzian) contributions are separately shown. The measured resolution function is presented on the expanded scale in the inset.

$$S_{\text{qe}}(Q, \omega) = \frac{\hbar\omega/k_B T}{1 - \exp(-\hbar\omega/k_B T)} \times \left[\frac{a_0(Q)}{\pi} \frac{\Gamma_0(Q)}{\omega^2 + \Gamma_0^2(Q)} + \frac{a_1(Q)}{\pi} \frac{\Gamma_1(Q)}{\omega^2 + \Gamma_1^2(Q)} \right],$$

$$S_{\text{inel}}(Q, \omega) = [n(\omega) + 1]a_c(Q) \times \frac{\Gamma_c(Q, \omega)}{[\omega^2 - \omega_c^2(Q)]^2 + \Gamma_c^2(Q, \omega)};$$

$n(\omega)$ is the Bose factor, $\Gamma_0(Q)$ was assumed equal to DQ^2 , and $\Gamma_1(Q)$, $\Gamma_c(Q, \omega)$, $\omega_c(Q)$, $a_0(Q)$, $a_1(Q)$, and $a_c(Q)$ were left as free parameters. The number of fitting parameters was further reduced by assuming the damping function $\Gamma_c(Q, \omega)$, which is always an odd function of ω , given by $\Gamma_c(Q, \omega) = \alpha Q \omega$. This expression is consistent with the random phase approximation to the dynamic structure factor of a liquid metal treated as the two-component mixture of interacting electrons and ions [1]. The convolution of $S(Q, \omega)$ with the four-dimensional (\mathbf{Q}, ω) -dependent resolution function was fitted to the experimental data. The results of the fit turned out to be satisfactory at all the

measured wave vectors and independent of the inelastic contribution for Q greater than 0.6 \AA^{-1} . As to the free parameters of the fit, we found that $\Gamma_1(Q)$ has a small Q dependence, whereas $\omega_c(Q)$ shows an almost linear trend up to $Q = 0.6 \text{ \AA}^{-1}$. Therefore, the fit of all the measured spectra was repeated assuming Γ_1 to be a constant and $\omega_c(Q) = c_0 Q$, c_0 being the collective mode velocity. In this way, the fit was carried out by using the three Q -independent parameters Γ_1 , c_0 , and α and the three amplitudes $a_0(Q)$, $a_1(Q)$, and $a_c(Q)$.

The best fit curves are shown in Fig. 1 in comparison with the experimental data. The following best fit values of the Q -independent parameters were obtained: $\hbar\Gamma_1 = 2.0 \pm 0.2 \text{ meV}$, $\hbar c_0 = 13.8 \pm 0.5 \text{ meV/\AA}^{-1}$, and $\hbar\alpha = 9 \pm 2 \text{ \AA meV}$. The energy integrals of the narrow, $A_0(Q)$, and the broad, $A_1(Q)$, quasielastic components and of the inelastic component, $A_c(Q)$, are shown in Fig. 2. In the present Q range, $A_c(Q)$ is almost constant and close to the static structure factor of liquid mercury. This is an indication that the quasielastic structure of the spectrum is almost entirely due to the self-dynamics. The integrals $A_0(Q)$ and $A_1(Q)$ are, respectively, a slightly decreasing and an increasing function of Q , although the present Q range was not wide enough to detect a possible saturation of $A_1(Q)$. This finding could be interpreted as an evolution of the self-dynamics from the hydrodynamic regime, characterized by $\Gamma_0(Q)$, to a local regime, as represented by the broad Γ_1 Lorentzian. This suggests that, in this intermediate Q range, the single-particle behavior of the system is intermediate between the two regimes. Modeling the sharp quasielastic peak by means of the $\Gamma_0(Q)$ Lorentzian was a noninfluential choice, since the effective width and shape of this peak were masked completely by the resolution. The Γ_1 Lorentzian, on the contrary, was broader than the resolution, the width Γ_1 was essentially Q independent, and $1/\Gamma_1$ was $\sim 0.3 \text{ ps}$. These characteristics cannot be attributed to a free diffusion in real space and suggest the presence of a fast

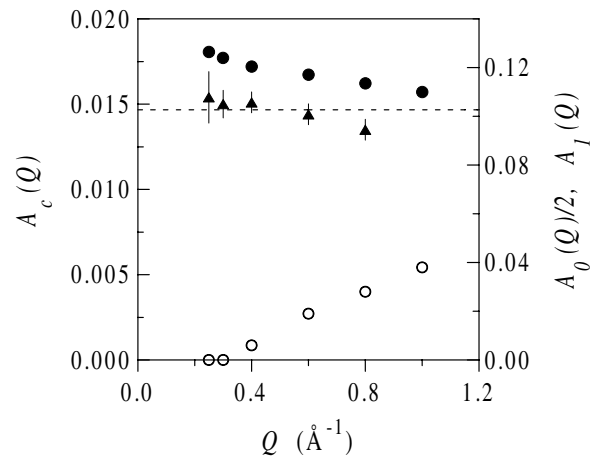


FIG. 2. $A_0(Q)$ (dots), $A_1(Q)$ (circles), and $A_c(Q)$ (triangles) versus Q (see text).

time-scale contribution in the self-dynamics of mercury. Indeed, $1/\Gamma_1$ could be interpreted as the equivalent of a "residence" time associated with a localized motion of a single atom.

As to the collective dynamic behavior, the present study has the merit of showing that well-defined inelastic propagating modes exist in mercury up to wave-vector transfer values $Q \sim 0.6 \text{ \AA}^{-1}$, with an associated velocity equal to $2100 \pm 80 \text{ m/s}$, as obtained from the linear low- Q region of the dispersion curve $\hbar\omega_c(Q)$. This value largely exceeds the sound velocity (1451 m/s) measured in liquid Hg at 293 K by ultrasound spectroscopy [13]. We interpreted the observed frequency of the collective excitations by means of the BS model [11] which had been successfully employed in the case of liquid alkali metals [6]. This model, which portrays the liquid metal as a gas of pointlike ions interacting through the Coulomb potential screened by the electron gas, results in the well-known long-wavelength approximation for the frequency of the longitudinal collective excitations; that is

$$\omega^2(Q) = \frac{\Omega_p^2}{\epsilon(Q)}, \quad (1)$$

where $\Omega_p^2 = 4\pi n e^2 / M$ is the plasma frequency of the ion gas, n and M being the number density and the mass of the ion. $\epsilon(Q)$ is the (static) dielectric function of the homogeneous electron gas at the appropriate density $\rho = Z^{1/3}n$, Z being the ionic charge. The BS model was applied to liquid mercury using $Z = 2$ and $\epsilon(Q)$ obtained from the Lindhart formula [11]. The resulting velocity was $\lim_{Q \rightarrow 0} \sqrt{\frac{\Omega_p^2}{\epsilon(Q)Q^2}} = 2090 \text{ m/s}$, that is higher than the sound velocity and coincident with the experimental value associated to the collective excitations. This result shows that the BS model still accounts for the long-wavelength collective behavior in a system such as mercury. As a further check, we applied the same model to the published data on liquid lead [12]. By using $Z = 1.8$, as calculated in Ref. [17] for solid fcc Pb, we found a velocity of 1760 m/s , that is a value again coincident with that observed in the neutron scattering measurement [12].

Equation (1) provides a good approximation for the velocity of the density fluctuation excitations in systems as different as alkali and polyvalent metals and, as recently reported, lithium ammonia at the solubility limit [8], where r_s varies from 5.37 in Rb to 2.70 in Hg to 7.4 in $\text{Li}(\text{NH}_3)_4$. This suggests that the main interaction governing the propagation of collective modes is the Coulomb potential screened by the electron gas. Indeed, the pointlike approximation for the ion core contained into the BS model confines the repulsion core potential to a negligible role. The most intriguing result of the present investigation is the very high ratio between the collective excitation velocity and the sound velocity in liquid mercury, that is the remarkable anomalous dispersion of the longitudinal density fluctuation modes. Actually, anomalous dispersion has

been often observed in metals, but an impressively large effect as the present one has been reported only in water [18], that is in a profoundly different system. As a conclusion, we want to stress once more that although the discussed systems, namely alkali metals, mercury and lead, have very different ionic core characteristics, the velocity of the collective modes was found to be well reproduced by the BS model, that is a model which emphasizes the role of the electron density. Therefore, one can conjecture that the repulsive ionic core has a main role in determining the sound velocity, whereas the presence of the anomalous dispersion is brought about by the interplay between electronic screening and shape of the ionic core.

-
- [1] N. H. March, *Liquid Metals* (Cambridge University Press, Cambridge, 1990).
 - [2] J.-B. Suck, *Int. J. Mod. Phys. B* **7**, 3003 (1993).
 - [3] J. R. D. Copley and J. M. Rowe, *Phys. Rev. Lett.* **32**, 49 (1974); J. R. D. Copley and J. M. Rowe, *Phys. Rev. A* **9**, 1656 (1974).
 - [4] T. Bodensteiner, Chr. Morkel, W. Gläser, and B. Dorner, *Phys. Rev. A* **45**, 5709 (1992).
 - [5] F. J. Bermejo *et al.*, *Phys. Rev. E* **56**, 3358 (1997); F. J. Bermejo *et al.*, *Phys. Rev. Lett.* **85**, 106 (2000).
 - [6] L. E. Bove, F. Sacchetti, C. Petrillo, and B. Dorner, *Phys. Rev. Lett.* **85**, 5352 (2000).
 - [7] H. Sinn *et al.*, *Phys. Rev. Lett.* **78**, 1715 (1997); T. Scopigno, U. Balucani, G. Ruocco, and F. Sette, *Phys. Rev. Lett.* **85**, 4076 (2000); T. Scopigno, U. Balucani, G. Ruocco, and F. Sette, *Phys. Rev. E* **63**, 011210 (2001).
 - [8] C. A. Burns *et al.*, *Phys. Rev. Lett.* **86**, 2357 (2001).
 - [9] H. Mori, *Prog. Theor. Phys.* **33**, 423 (1965); D. Levesque, J. Verlet, and J. Kurkijarvi, *Phys. Rev. A* **7**, 1690 (1973).
 - [10] U. Balucani and M. Zoppi, *Dynamics of the Liquid State* (Clarendon Press, Oxford, 1994).
 - [11] D. Pines and Ph. Nozieres, *The Theory of Quantum Liquids* (W. A. Benjamin, Inc., New York, 1966).
 - [12] O. Soderstrom, J. R. D. Copley, J.-B. Suck, and B. Dorner, *J. Phys. F* **10**, L151 (1980).
 - [13] D. R. Lide, *CRC Handbook of Chemistry and Physics* (CRC Press, Inc., New York, 1997).
 - [14] C. Petrillo and F. Sacchetti, *Acta Crystallogr. Sect. A* **46**, 440 (1990).
 - [15] S. W. Lovesey, *Theory of Neutron Scattering from Condensed Matter* (Oxford University Press, Oxford, 1986), Vol. 1.
 - [16] M. J. Cooper and R. Nathans, *Acta Crystallogr.* **23**, 357 (1967); B. Dorner, *Acta Crystallogr. Sect. A* **28**, 319 (1972).
 - [17] D. A. Papacostantopoulos, *Handbook of the Band Structure of Elemental Solids* (Plenum Press, New York, 1986).
 - [18] J. Teixeira, M. C. Bellissent-Funel, S. H. Chen, and B. Dorner, *Phys. Rev. Lett.* **54**, 2681 (1985); G. Ruocco *et al.*, *Nature* (London) **379**, 521 (1996); C. Petrillo, F. Sacchetti, B. Dorner, and J.-B. Suck, *Phys. Rev. E* **62**, 3611 (1999).